LETTER

ACS chemical biology

# Analysis of Protein Complex Hierarchy in Living Cells

**Alen Piljić and Carsten Schultz***

Gene Expression Unit, European Molecular Biology Laboratory, Meyerhofstr. 1, 69117 Heidelberg, Germany

**ABSTRACT** The identification and analysis of protein complexes is usually achieved by performing *in vitro* experiments. We describe a translocation-based method for studying protein complexes in living cells. Annexin A4, a phospholipid- and calcium-binding protein, translocates from the cytoplasm and nucleoplasm to plasma and nuclear membranes in response to elevated intracellular calcium levels. By fusing a bait protein, for instance, a core component of a protein complex or a similarly relevant peptide, to the annexin, translocation of both bait and its interacting target proteins are readily monitored in living cells in response to a single treatment. Proteins of interest are fused to a variety of fluorescent proteins suitable for multiparameter imaging. Using this generally applicable approach, we were able to visualize the formation of protein complexes in their natural environment. Specifically, we detected the hierarchical assembly of four-component protein complexes in single cells.

Protein−protein interactions are crucial for virtually all cellular processes. It is therefore not surprising that protein−protein interaction and protein complex analysis is becoming increasingly important in molecular biology, biochemistry, and computational biology (*1, 2*). Furthermore, compromised protein−protein interactions can contribute to diseases, which makes identification of protein−protein interaction inhibitors highly desirable in drug discovery (*3*). There are different ways protein−protein interactions can be identified and characterized. Among the most common experimental methods are yeast two-hybrid, tandem affinity purification, and mass spectrometry, as well as co-immunoprecipitation and PCA (protein-fragment complementation assays) (*1, 4*). Although these methods are irreplaceable, additional, especially fluorescent, tools that allow monitoring of protein−protein interactions in living cells are very desirable and need to be developed. Techniques such as FRET (fluorescence resonance energy transfer) (*5*) and BiFC (bimolecular fluorescence complementation) (*6*) are regularly employed, each having advantages and drawbacks. For instance, optimization of constructs for FRET applications is notoriously difficult (*7*). The same is in many cases true for BiFC (*6*) because both methods require a particular distance and orientation of the fluorescent protein components for optimal performance. In addition, fluorescent techniques used to date have been mostly limited to binary interactions.

As an alternative, translocation-based methods have been described for detecting protein−protein interactions in living cells (*8*–*12*). These methods use baits fused to proteins that, for instance, change distribution within the cell following a stimulus. Upon translocation to a particular cellular compartment, proteins interacting with the bait have to follow. Usually, relocation of protein fusions is monitored with the help of fluorescent proteins. Translocation-based methods require little construct optimization and are robust, fast, flexible, and mostly reversible, which makes them suitable for the discovery of small molecule protein interaction inhibitors in high-throughput setups (*9, 10*). Of course, membrane-associated or transmembrane proteins are not suitable for detection by translocation. Most of the existing translocation methods require that both bait and target localize to a particular cell region (*e.g.*, being exclusively cytosolic or nuclear) (*8, 9, 12*). Our goal was to develop a method for detecting interactions of soluble proteins having no restriction in protein localization but providing the ability to observe multicomponent protein complexes.

The assay described here relies on the calcium-induced translocation of a bait protein fused to annexin A4. Massively elevated calcium levels, for example, after addition of the ionophore ionomycin, induce complete translocation of the annexin from the cytoplasm and nucleoplasm to the plasma membrane and nuclear membrane, respectively. Additionally, membranes in the peri-

*Corresponding author, schultz@embl.de.

Received for review July 30, 2008 and accepted October 29, 2008.

Published online November 24, 2008

10.1021/cb8002539 CCC: $40.75

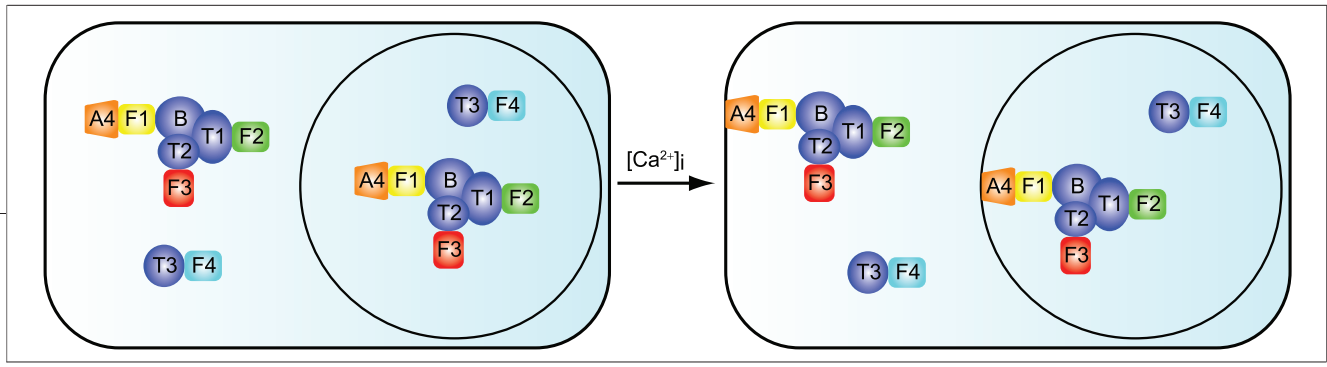


**Figure 1. Schematic view of the translocation-based protein−protein interaction and protein complex analysis assay. Annexin A4 serves as a calcium-dependent membrane anchoring unit that forces the bait protein and any interacting partner to translocate, while non-interacting proteins remain soluble. A4 = annexin A4, B = bait, T1−3 = targets, F1−4 = fluorescent proteins.**

nuclear region and vesicles are targeted by annexin A4 in some cells, as previously observed (*13*). The completeness of translocation makes the event unambiguous and bait translocation irreversible. Target proteins follow the bait only in case of interaction. Translocations of both annexin A4-bait and target proteins are easily monitored when spectrally distinguishable fluorescent proteins are fused to each of the complex components (Figure 1).

We selected different protein complexes relevant to signal transduction, including PI3K, NFκB, and CDK2, and prepared constructs for transfection into mammalian cells. We initially focused on binary interactions. Each of the components was N-terminally fused to a fluorescent protein. In addition, the bait was connected to annexin A4. The resulting constructs would thus encode for instance A4-EYFP-bait and ECFP-target. These constructs were then transfected into N1E-115 neuroblastoma cells. The latter are particularly convenient for imaging of translocation events by confocal microscopy as a result of their high pyramidal shape. Some experiments were performed in HeLa cells with essentially identical results. In the range of 24−48 h post-transfection we acquired images using a Leica TCS SP2 AOBS microscope (Leica Microsystems) with an HCX PL APO lbd.BL 63.0x 1.40 oil objective at 22 °C. The calcium ionophore ionomycin (Calbiochem) at 10 μM was used to elevate intracellular calcium concentration. First, each of the constructs was transfected separately, and images were acquired before and approximately 5 min after ionomycin addition. By this way, we confirmed translocation of the annexin-bait fusion and target indifference to the calcium rise (see Supplementary Figure 1). Next, bait and target constructs were co-transfected. The bait fusion translocated completely, whereas the target translocation depended on the degree of interaction between the proteins. Interactions were classified as positive if clear plasma or nuclear membrane staining was observed in the target channel following ionomycin treatment and if the fluorescence signal measured in the membranes was significantly higher than the residual cytoplasmic or nuclear staining (at least three times standard deviation of mean residual fluorescence). One example features N1E-115 cells expressing p110α (PIK3CA, catalytic subunit α of the PI 3-kinase) acting as bait and p85α (PIK3R1, regulatory subunit α of the PI 3-kinase) acting as target. Both fusions were cytosolic and translocated to the plasma membrane upon elevation of intracellular calcium (Figure 2, panel a). The experiment worked equally well if target-bait roles were exchanged (see Supplementary Figure 2). When p50 (amino acids 1−433 of p105, NFKB1) and p65 (RELA) of the NFκB complex were used as bait and target, respectively, we observed their interaction in the nucleus where both proteins were present. p50 was absent from the cytosol and p65 therefore did not translocate in this compartment (Figure 2, panel b). We also monitored interaction of catalytic subunits of protein phosphatase 1 with their regulatory subunits. In Figure 2, panel c, we show translocation of inhibitor-2 (PPP1R2, regulatory subunit of protein phosphatase 1, PP1) acting as bait and co-translocation of the protein phosphatase PP1γ (PPP1CC, catalytic subunit γ of PP1) acting as target. Additional PP1 and NFκB interaction experiments, including p65 interaction with p105, IκB, or both, are listed in Table 1, and images are included in Supplementary Figure 2. To evaluate the specificity of the assay, we tested several combinations of non-interacting proteins. In none of these experiments was target translocation observed, implying high specificity of detected protein−protein interactions. Three examples of such experiments are shown in Figure 2, panels d−f, and additional experiments are included in Supplementary Figure 3.

In most two-component protein complex analysis experiments, we used ECFP and EYFP as fluorescent protein labels. The emission and excitation settings were ECFP ex 458 nm, em 465−495 nm; EYFP ex 515 nm, em 530−550 nm. In order to study larger complexes, we introduced additional fluorescent proteins. The third component was typically labeled with mCherry and the fourth with EGFP. The imaging settings in these experiments were similar to those known from previous multicolor applications (*14, 15*): ECFP ex 405 nm, em 450−480 nm; EGFP ex 488 nm, em 495−510 nm; EYFP ex 532 nm, em 545−565 nm; mCherry ex 594 nm, em 605−650 nm. These fluorescent proteins and settings enabled us to analyze a four-component complex. We chose a known complex between CDK2, cyclin A1 (CCNA1), p21 (CDKN1A), and PCNA and prepared bait and target constructs as described above. A series of experiments was performed to determine if complex formation can be observed in a way that would be expected from the literature, according to which interaction between CDK2-cyclin A1 complex and PCNA is mediated by p21 protein (*16*). We used CDK2 as bait and first demonstrated its interaction with cyclin A1 (Figure 3, panel a). We then added PCNA to the system but observed no interaction with CDK2-cyclin A1

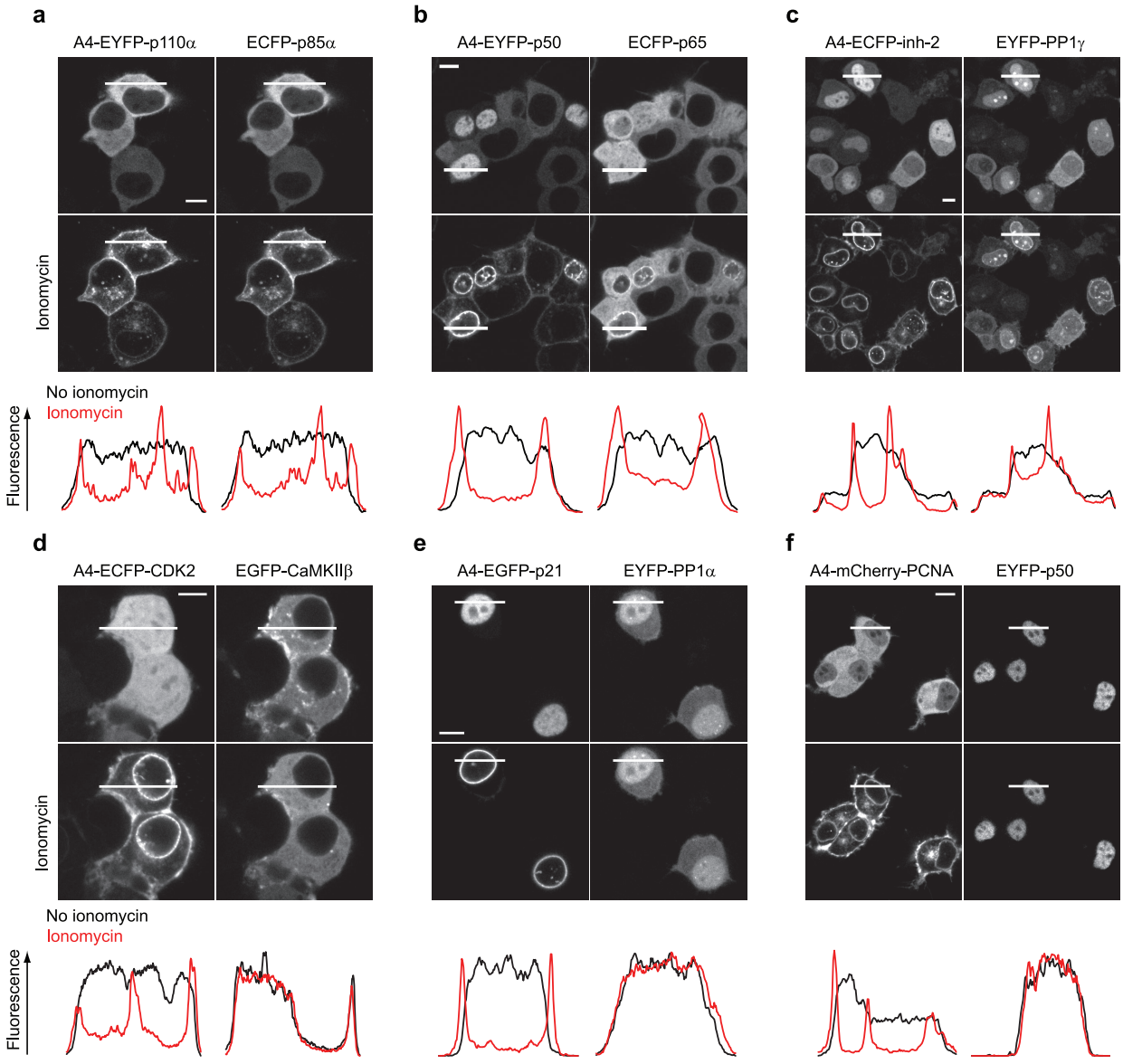


**Figure 2. Examples of experiments involving two interacting or non-interacting proteins. Known interacting protein pairs: a) N1E-115 cells expressing the catalytic p110α and the regulatory p85α subunit of PI 3-kinase. Translocation in both emission channels upon addition of ionomycin indicates protein−protein interaction. White lines indicate the position of the measured fluorescence profiles that are shown in the graphs below the corresponding images. b) Interaction of p50 and p65 of the NFκB complex in N1E-115 cells. c) Interaction of a catalytic (PP1γ) and a regulatory (inhibitor-2) subunit of protein phosphatase 1 (PP1) in N1E-115 cells. Known non-interacting protein pairs: d) The lack of translocation in the CaMKIIβ channel indicates there is no interaction with CDK2. e) No interaction in N1E-115 cells is observed between p21 (CDKN1A) and catalytic (PP1α) subunit of protein phosphatase 1 (PP1). f) No interaction in N1E-115 cells is observed between PCNA and p50 (aa 1−433 of p105, NFKB1). All scale bars are 10 μm.**

**TABLE 1. Protein complexes analyzed using the multicolor translocation-based assay; targets interacted with the bait unless stated otherwise**

| Complex | Bait | Targets |
|---|---|---|
| PI3K | p110α | p85α |
| | p85α | p110α |
| | IRS1 | p110α (no interaction) |
| | IRS1 | p85α |
| | IRS1 | p110α, p85α |
| NFκB | p65 | p105 |
| | p65 | p105 (C-terminal fusion) |
| | p65 | IκB |
| | p65 | IκB, p105 |
| | p65 | IκB, p105 (C-term) |
| | p50 | p65 |
| PP1 | Inhibitor-1 | PP1α |
| | Inhibitor-2 | PP1α |
| | PP1α | Inhibitor-2 |
| | Inhibitor-1 | PP1α |
| | Inhibitor-2 | PP1α |
| | PP1γ | Inhibitor-2 |
| CaMKII | CaMKIIα | CaMKIIα |
| | CaMKIIβ | CaMKIIβ |
| | CaMKIIα | CaMKIIβ |
| | Calmodulin | CaMKIIα, CaMKIIβ |
| CDK2-cyclin A1-p21-PCNA | CDK2 | cyclin A1 |
| | CDK2 | cyclin A1, PCNA (no interaction) |
| | CDK2 | p21, PCNA |
| | CDK2 | cyclin A1, p21, PCNA |
| | p21 | cyclin A1 (or CDK2, or PCNA) |
| | p21 | CDK2, cyclinA1 |
| | p21 | CDK2, PCNA |
| | p21 | cyclin A1, PCNA |
| | p21 | CDK2, cyclin A1, PCNA |
| p53-MDM2 | p53 | MDM2 |
| | p53 (C-term) | MDM2 (C-term) |
| | FWL peptide | MDM2 |
| SH3-APTpep | SH3(Abl1) | APT peptide |

(Figure 3, panel b). When p21 was used in combination with CDK2 and PCNA and cyclin A1 was left out, translocation of both targets was observed, thus confirming the bridging function of p21 (Figure 3, panel c). When we introduced all components in a single cell, formation of the entire four-protein complex was observed (Figure 3, panel d). Finally, we used p21 as bait and confirmed its interaction with all components of the complex individually, including interaction with cyclin A1, and all possible combinations (Table 1). The experiments demonstrate that the hierarchy of the complex is (CDK2-cyclin A1)-p21-(PCNA).

The interaction hierarchy of PI 3-kinase with IRS1 was investigated in a similar way. IRS1 interacted with p85α (PIK3R1) but lacked association with p110α (PIK3CA). In the presence of p85α, IRS1 also pulled p110α to the membrane due to interaction of p110α and p85α (Table 1 and Supplementary Figure 2) (*17*). More results of other protein complexes and interactions (including CaMKII and p53-MDM2) are summarized in Table 1, and representative images of translocations are included in Supplementary Figure 2.

In addition to protein complex analysis, the translocation assay may be used in protein–peptide interaction studies. As an example, we used a peptide originating from p53 (FWL peptide QET**F**SDL**W**KL**L**PEN, $K_d$ = 0.4 μM) as bait that targeted MDM2 (*18*) (Table 1 and Supplementary Figure 2) and demonstrated the interaction of the SH3 domain of Abl1 and a 10-mer polyproline peptide (APT peptide **APT**YSPPPPP, $K_d$ = 0.4 μM) (*19*) (Table 1 and Supplementary Figure 2). Finally, we used the known p53-MDM2 interaction inhibitor nutlin-3 (*20*) and achieved partial reversion of translocation of the target while leaving the bait unaffected (Supplementary Figure 4). The experiment implies the potential use of the method in detecting inhibitors of protein–protein interactions in high-throughput setups, a subject we will exploit in the future. Additionally, the method may also be used to discover previously unknown protein–protein interactions. This requires the availability of larger libraries of genes fused to fluorescent proteins and a more automated microscopy setup including automated image analysis software.

In the interaction experiments presented here, we mostly used N-terminal fusions but observed no difference when C-terminal fusions were used (*e.g.*, p53-MDM2, Supplementary Figure 2). Since the fused tag may sterically hinder some interactions, both types of fusions should be tested. Fusions were sufficiently overexpressed to prevent potential interference of comparably low-expressing endogenous proteins. However, experiments with target and bait in exchanged roles often resulted in an unequal degree of target translocation (data not shown). Typically, the smaller of the interacting partners performed better as bait, probably the result of stronger expression levels of the smaller construct. Better target translocation is expected if more bait than target fusion is expressed in cells. In cases where the target protein is expressed in large excess of the bait, false negative responses might be the result. We therefore attempted to keep the expression levels as even as

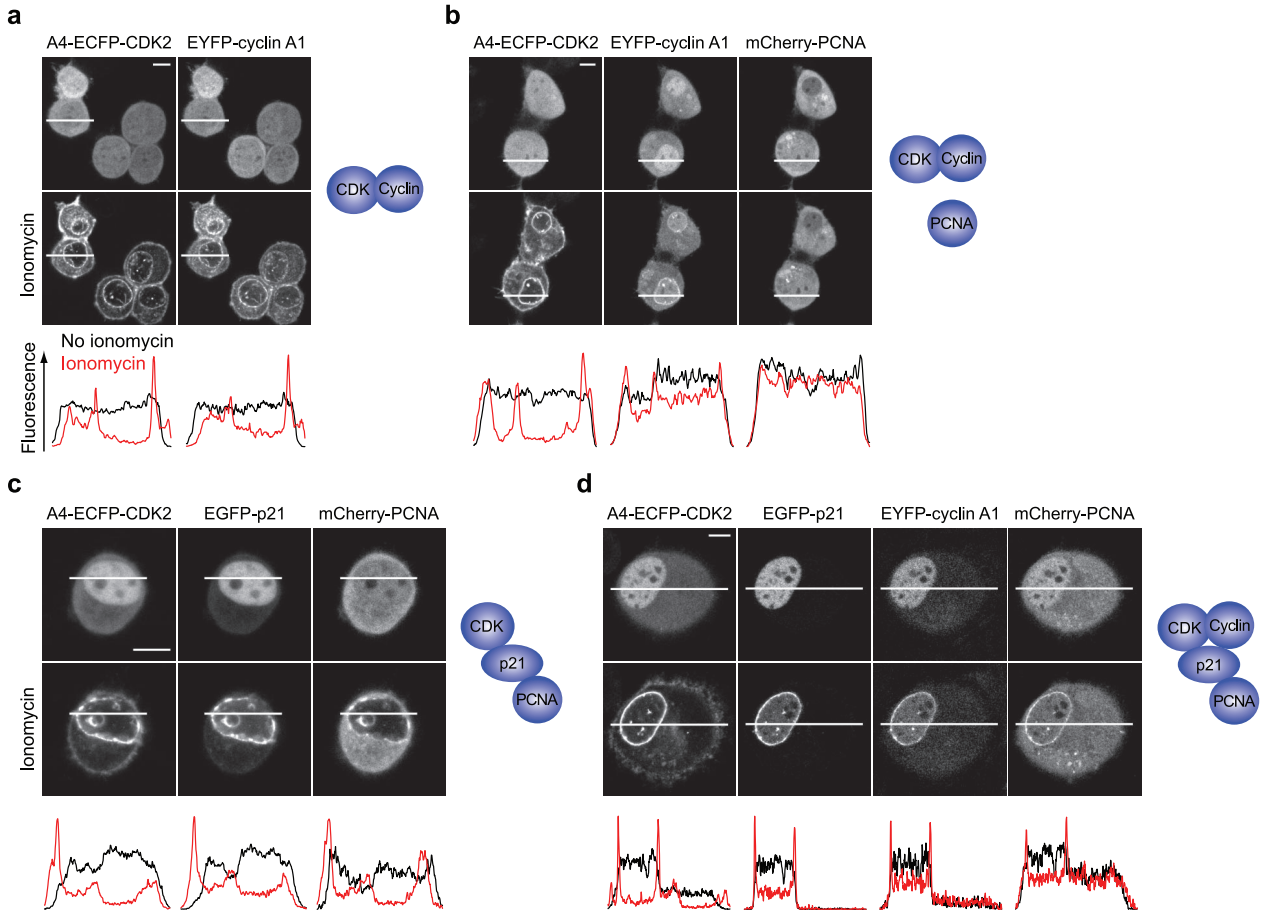


**Figure 3. Translocation-based four-component protein complex detection in N1E-115 cells. a) Cells expressing CDK2 (bait) and cyclin A1 (target) before and after ionomycin stimulation. Graphs below images show fluorescence profiles measured in the sections indicated by the white lines. b) Cells and fluorescence profiles demonstrating interaction between CDK2 and cyclin A1, but no interaction with PCNA. c) Cells and fluorescence profiles demonstrating interaction of CDK2 and PCNA in the presence of p21. d) Cells are shown that express all four components of the complex. Their interaction is evidenced by translocation to the nuclear membrane and emphasized by fluorescence profiles depicted below respective cell images. All scale bars are 10 μm.**

possible (see Methods) or to have the bait in slight excess. From our examples with peptides serving as bait or target, we can estimate that submicromolar binding constants will likely be sufficient for successful co-translocation. When we tested peptides with a $K_d > 10$ μM, such as a translin-interacting peptide (VSVSPARVYSPV, $K_d$ = 43 μM) (*21*) binding to translin, we observed no co-translocation (data not shown). We did not see a significant difference in localization of proteins acting as baits or targets, indicating annexin A4 inertness in calcium absence (Supplementary Figure 1). Interacting proteins were mostly soluble, cytosolic and/or nuclear. In two cases we observed partial membrane staining of the targets prior to calcium elevation (PP1α and CaMKIIβ, Supplementary Figures 1 and 2), but a few minutes after calcium stimulation both proteins relocated to the cytosol and could therefore still be used in the experiments. Although in some cases a high calcium signal in cells may disrupt interactions or may lead to translocation due to the presence of C2 domains, calcium did not seem to negatively influence the interactions examined here. In fact, for calmodulin interaction with CaMKII, high calcium levels were beneficial (Supplementary Figure 2).

The annexin A4 based assay described here is easy to handle, quick to apply to living cells once the proteins of interest are flu-

orescently tagged, and widely applicable and robust. Apart from performing both C- and N-terminal labeling, which may be necessary in some cases, no tedious and systematic construct optimization is needed. A set of basic vectors enables efficient cloning of target and bait constructs labeled with different fluorescent proteins. Once settings are defined, microscopy is straightforward and fast with an experiment taking on average 15−20 min. Annexin A4 has only a few reported interacting partners (*22, 23*), a positive feature that limits potentially false positive results. None of the target proteins that we tested co-translocated with annexin A4-fluorescent protein lacking the bait, indicating that no interaction with annexin A4 itself (or the fluorescent protein) was taking place (data not shown). Further, we tested over 15 different combinations of non-interacting proteins and observed no target translocation, demonstrating high assay specificity (Figure 2, panels d−f, and Supplementary Figure 3). Annexin A4 is uniformly distributed in cells, is long-lived, and appears to be inert. In unstimulated cells, annexin-bait fusion in most cases showed the localization of the bait protein (Supplementary Figure 1). Only in a few cases, smaller proteins were found with reduced nucleosolic location when they were additionally fused to annexin. In contrast to most other fluorescent translocation assays, interacting partners can be nuclear and/or cytosolic (*8, 9, 12*), provided they are soluble. Annexin's change in distribution following a stimulus is complete, leading to full removal of fluorescence from the cytosol (*13, 14*). The lack of relocation is beneficial for assay sensitivity. Finally and most importantly, our approach was able for the first time to analyze protein complexes consisting of four or potentially more components and to determine the hierarchy of the complex in living cells. With the increasing general availability of user-friendly confocal microscopes capable of multicolor imaging, we believe that the easy-to-use method described here will soon become an important tool for the analysis of protein complexes and their assembly.

## METHODS

**Cloning.** pECFP-C1/N1, pEYFP-C1/N1, and pEGFP-C1/N1 are former Clonetech vectors. ECFP contained mutations described in Llopis et al. (*24*). pmCherry-C1/N1 were created by subcloning of mCherry from pmCherry-N1-Annexin A4 vector (*25*) into pEYFP-C1/N1 vectors using AgeI and BsrGI restriction enzymes.

pA4-ECFP-C1 and pA4-EYFP-C1 were created by amplifying annexin A4 and inserting into pECFP-C1 and pEYFP-C1 using NheI and AgeI. pECFP-A4-N1 and pEYFP-A4-N1 were created by PCR amplification and insertion of annexin A4 using BsrGI and NotI. pA4-mCherry-C1 and pmCherry-A4-N1 were created by subloning of mCherry from pmCherry-N1-Annexin A4 vector into pA4-EYFP-C1 and pEYFP-A4-N1 vectors using AgeI and BsrGI. pA4-EGFP-C1 and pEGFP-A4-N1 were created by subcloning of EGFP from pEGFP-C1 vector into pA4-EYFP-C1 and pEYFP-A4-N1 vectors using AgeI and BsrGI.

The basic set of vectors described above enabled cloning of a desired protein in four different colors with or without annexin A4 to serve as bait or target, respectively. All C1 or N1 vectors, respectively, had the same multicloning site so that the proteins could be amplified in a single PCR and inserted in any desirable vector. The cloning of baits and targets is described in Supporting Information.

**Cell Culture and Transfection.** All cell experiments were performed with N1E-115 neuroblastoma and HeLa cells. Cells were passaged and maintained in DMEM supplemented with 10% FBS and 0.1 mg $mL^{-1}$ primocin. For imaging experiments, cells were plated in 35 mm MatTek chambers (MatTek Corporation) and transfected at around 50% confluency with FuGENE 6 reagent (Roche). Transfections were performed in Opti-MEM (Gibco) according to the manufacturer's instructions. For multiple transfections, equal amounts of DNA were used for each construct. Cells were washed 24−48 h after transfection and incubated in imaging medium (20 mM Hepes, pH 7.4, 115 mM NaCl, 1.2 mM $CaCl_2$, 1.2 mM $MgCl_2$, 1.2 mM $K_2HPO_4$, 2 g $L^{-1}$ D-glucose) at 37 °C with 5% $CO_2$ for ~30 min before imaging. A DMSO stock of ionomycin (Calbiochem) was prepared and ionomycin prediluted in imaging medium before it was carefully added to the dish to give a final concentration of 10 μM.

**Equipment and Settings.** All experiments were performed on a Leica TCS SP2 AOBS microscope (Leica Microsystems). We used an HCX PL APO lbd.BL 63.0x 1.40 oil objective. The pinhole was half-opened in all experiments (2.62 airy). Excitation and emission settings are described in the main text and were kept constant. In brief: CFP/YFP, CFP excitation 458 nm, emission 465−495 nm, YFP excitation 515 nm, emission 530−550 nm; CFP/YFP/mCherry, CFP excitation 458 nm, emission 465−495 nm, YFP excitation 515 nm, emission 530−550 nm, mCherry excitation 594 nm, emission 605−650 nm; CFP/GFP/YFP, CFP excitation 405 nm, emission 450−480 nm, GFP excitation 488 nm, emission 495−510 nm, YFP excitation 532 nm, emission 545−570 nm; CFP/GFP/YFP/mCherry, CFP excitation 405 nm, emission 450−480 nm, GFP excitation 488 nm, emission 495−510 nm, YFP excitation 532 nm, emission 545−565 nm, mCherry excitation 594 nm, emission 605−650 nm.

Laser power and PMT gain were adjusted from experiment to experiment. Images were taken in 8 bit mode, with 2−4 line averaging, before ionomycin addition and about 5′ after addition of 10 μM ionomycin.

Microscope settings were calibrated to approximate the relative expression levels of the bait and target by transfecting the cells with vectors encoding single fluorescent proteins under identical promoters (pECFP-C1, pEYFP-C1, pEGFP-C1, and pmCherry-C1) which are, despite variability between cells, on average fairly equally expressed. Alternatively and more accurately, to estimate expression levels of ECFP and EYFP fusions, in some cases we used the ECFP-EYFP construct CYNEX4 (*13*), in which ECFP and EYFP are in 1:1 ratio. When using this type of intramolecular sensors, we took into account the donor quenching due to FRET (35%). Alternatively, constructs combining other fluorescent proteins in a single fusion could be used to achieve more precise calibration in experiments with three, four or more fluorescent proteins.

**Image Processing.** All image processing and calculations were performed using ImageJ (http://rsb.info.nih.gov/ij/). Background level was measured outside cells and subtracted globally. Median filter (1 pixel) was used for image smoothening and brightness/contrast was adjusted.

*Acknowledgment:* We thank EMBL's Advanced Light Microscopy Facility for technical advice, H. Stichnoth for cultured cells, R. Tsien (UCSD) for mCherry, T. Meyer (Stanford) for CaMKII, J. Schmid (Vienna) for p65, and R. Russell (EMBL Heidelberg) for PP1γ and Abl1 cDNA. The work was supported by the EU 6.FP Integrated Project "Molecular Imaging" LSHG-CT-2003-503259 and the Helmholtz Initiative for Systems Biology "SBCancer".

*Supporting Information Available:* This material is free *via* the Internet.

## REFERENCES

1. Shoemaker, B. A., and Panchenko, A. R. (2007) Deciphering protein-protein interactions. Part I. Experimental techniques and databases, *PLoS Comput. Biol. 3*, 337–344.
2. Shoemaker, B. A., and Panchenko, A. R. (2007) Deciphering protein-protein interactions. Part II. Computational methods to predict protein and domain interaction partners, *PLoS Comput. Biol. 3*, 595–601.
3. Arkin, M. R., and Wells, J. A. (2004) Small-molecule inhibitors of protein-protein interactions: progressing towards the dream, *Nat. Rev. Drug Discovery 3*, 301–317.

4. Michnick, S. W., Ear, P. H., Manderson, E. N., Remy, I., and Stefan, E. (2007) Universal strategies in research and drug discovery based on protein-fragment complementation assays, *Nat. Rev. Drug Discovery 6*, 569–582.
5. Jares-Erijman, E. A., and Jovin, T. M. (2003) FRET imaging, *Nat. Biotechnol. 21*, 1387–1395.
6. Kerppola, T. K. (2006) Visualization of molecular interactions by fluorescence complementation, *Nat. Rev. Mol. Cell Biol. 7*, 449–456.
7. Zhang, J., Campbell, R. E., Ting, A. Y., and Tsien, R. Y. (2002) Creating new fluorescent probes for cell biology, *Nat. Rev. Mol. Cell Biol. 3*, 906–918.
8. Heydorn, A., Lundholt, B. K., Praestegaard, M., and Pagliaro, L. (2006) Protein translocation assays: key tools for accessing new biological information with high-throughput microscopy, *Methods Enzymol. 414*, 513–530.
9. Knauer, S. K., Moodt, S., Berg, T., Liebel, U., Pepperkok, R., and Stauber, R. H. (2005) Translocation biosensors to study signal-specific nucleocytoplasmic transport, protease activity and protein-protein interactions, *Traffic 6*, 594–606.
10. Knauer, S. K., and Stauber, R. H. (2005) Development of an autofluorescent translocation biosensor system to investigate protein-protein interactions in living cells, *Anal. Chem. 77*, 4815–4820.
11. Maroun, M., and Aronheim, A. (1999) A novel *in vivo* assay for the analysis of protein-protein interaction, *Nucleic Acids Res. 27*, e4.
12. Shen, K., Teruel, M. N., Subramanian, K., and Meyer, T. (1998) CaMKIIbeta functions as an F-Actin targeting module that localizes CaMKIIalpha/beta heterooligomers to dendritic spines, *Neuron 21*, 593–606.
13. Piljic, A., and Schultz, C. (2006) Annexin A4 self-association modulates general membrane protein mobility in living cells, *Mol. Biol. Cell 17*, 3318–3328.
14. Skrahina, T., Piljic, A., and Schultz, C. (2008) Heterogeneity and timing of translocation and membrane-mediated assembly of different annexins, *Exp. Cell Res. 314*, 1039–1047.
15. Hutter, H. (2004) Five-colour *in vivo* imaging of neurons in *Caenorhabditis elegans*, *J. Microsc. 215*, 213–218.
16. Kontopidis, G., Wu, S. Y., Zheleva, D. I., Taylor, P., McInnes, C., Lane, D. P., Fischer, P. M., and Walkinshaw, M. D. (2005) Structural and biochemical studies of human proliferating cell nuclear antigen complexes provide a rationale for cyclin association and inhibitor design, *Proc. Natl. Acad. Sci. U.S.A. 102*, 1871–1876.
17. Kapeller, R., and Cantley, L. C. (1994) Phosphatidylinositol 3-kinase, *Bioessays 16*, 565–576.
18. Bernal, F., Tyler, A. F., Korsmeyer, S. J., Walensky, L. D., and Verdine, G. L. (2007) Reactivation of the p53 tumor suppressor pathway by a stapled p53 peptide, *J. Am. Chem. Soc. 129*, 2456–2457.
19. Pisabarro, M. T., and Serrano, L. (1996) Rational design of specific high-affinity peptide ligands for the Abl-SH3 domain, *Biochemistry 35*, 10634–10640.
20. Vassilev, L. T., Vu, B. T., Graves, B., Carvajal, D., Podlaski, F., Filipovic, Z., Kong, N., Kammlott, U., Lukacs, C., Klein, C., Fotouhi, N., and Liu, E. A. (2004) *In vivo* activation of the p53 pathway by small-molecule antagonists of MDM2, *Science 303*, 844–848.
21. Neduva, V., Linding, R., Su-Angrand, I., Stark, A., de Masi, F., Gibson, T. J., Lewis, J., Serrano, L., and Russell, R. B. (2005) Systematic discovery of new recognition peptides mediating protein interaction networks, *PLoS Biol. 3*, 2090–2099.
22. Willshaw, A., Grant, K., Yan, J., Rockliffe, N., Ambavarapu, S., Burdyga, G., Varro, A., Fukuoka, S., and Gawler, D. (2004) Identification of a novel protein complex containing annexin A4, rabphilin and synaptotagmin, *FEBS Lett. 559*, 13–21.
23. Kaetzel, M. A., Mo, Y. D., Mealy, T. R., Campos, B., Bergsma-Schutter, W., Brisson, A., Dedman, J. R., and Seaton, B. A. (2001) Phosphorylation mutants elucidate the mechanism of annexin IV-mediated membrane aggregation, *Biochemistry 40*, 4192–4199.
24. Llopis, J., Westin, S., Ricote, M., Wang, Z., Cho, C. Y., Kurokawa, R., Mullen, T. M., Rose, D. W., Rosenfeld, M. G., Tsien, R. Y., and Glass, C. K. (2000) Ligand-dependent interactions of coactivators steroid receptor coactivator-1 and peroxisome proliferator-activated receptor binding protein with nuclear hormone receptors can be imaged in live cells and are required for transcription, *Proc. Natl. Acad. Sci. U.S.A. 97*, 4363–4368.
25. Piljic, A., and Schultz, C. (2008) Simultaneous recording of multiple cellular events by FRET, *ACS Chem. Biol. 3*, 156–160.